

STOCHASTIC ANALYSIS OF GEOMETRIC IMAGE PROCESSING USING B-SPLINES

G.K. Rohde^{1*}, D.M. Healy, Jr.¹, C.A. Berenstein¹, A. Aldroubi², D. Rockmore³

¹ Department of Mathematics, University of Maryland, College Park, MD, USA. 20742.

² Mathematics Department, Vanderbilt University, Nashville, TN, USA. 37235.

³ Department of Mathematics, Dartmouth College, Hanover, NH. 03755.

ABSTRACT

We look at the problem of extracting geometric functions such as spatial transformations and curves delineating edges to sub-pixel accuracy from noisy, sampled data. We analyze the stochastic properties of continuous B-spline interpolation to show that, in general noisy circumstances, sub-pixel accuracy is not obtainable when using low degree B-splines. Results using magnetic resonance image (MRI) data are shown.

1. INTRODUCTION

Many modern image processing operations can be formulated as a variational energy optimization problem where the goal is to estimate a spatial function f (a function that takes an input parameter or coordinate and outputs an image coordinate) that minimizes (or maximizes) some integral equation operating on the intensity values of an image $I(\mathbf{x})$ (or set of images $I_1(\mathbf{x}), I_2(\mathbf{x}), \dots$):

$$f = \arg \min_{f'} \Psi(I_1(\mathbf{x}), I_2(\mathbf{x}), \dots, f') \quad (1)$$

where Ψ usually represents an integral over the spatial domain of the image(s). More details about function f are given later. Example of image processing applications that allow such interpretation include image registration, image segmentation, edge detection, model-based tracking, and others. The cost function above can be optimized directly by using a nonlinear optimization method. Alternatively, Euler-Lagrange equations for the problem can be derived, from which iterative solutions arise naturally. In practice, whether iterative solutions are derived based on Euler-Lagrange equations or direct nonlinear optimization, computational considerations lead to discretizations of the cost function. This is normally achieved by replacing any continuous integrals in (1) with finite sums.

In many applications, such as nonrigid biomedical image registration, and sub-pixel edge detection, it is desirable that the solution f to the equations above can be estimated to sub-pixel accuracy. To that end, researchers usually employ a continuous approximation model for the images being analyzed.

*Currently a Post Doctoral Associate at the Naval Research Laboratory, Washington, DC, USA. 20375.

In this article we look at the problem of solving functional optimization-based image processing problems to sub-pixel accuracy when the digital images contain noise. Specifically we look at the problem of obtaining accurate sub-pixel estimates for image registration problems as well as for edge detection. We investigate the performance of B-spline interpolators within this context and show that, because of inevitable system noise, low degree interpolators are generally not capable of achieving sub-pixel accuracy because they cause systematic local optima artifacts in $\Psi(\dots)$. We show that as the degree of the B-spline interpolator used increases, however, sub-pixel accuracy may be obtainable as the artifactual oscillations decrease in magnitude.

2. THEORY

2.1. Stochastic image model

We use a simple linear, additive noise, stochastic model for the image formation process:

$$S(\mathbf{q}) = \int W(\mathbf{x})\Upsilon(\mathbf{q} - \mathbf{x})d\mathbf{x} + e(\mathbf{q}) \quad (2)$$

where $S(\mathbf{x})$ is the measured image, $\mathbf{x} \in \mathbb{R}^d$, $\mathbf{q} \in \mathbb{Z}^d$ organized in an M^d grid, $W(\mathbf{x})$ the object being imaged, $\Upsilon(\mathbf{x})$ the transfer function of the imaging system, and d the dimension of the image. $e(\mathbf{q})$ is a zero-mean random variable representing the influence of noise sources (thermal, physiological, etc.), and it is statistically independent from the signal part of the image. Through simple substitution, it is trivial to show that the covariance matrix $R_S(\mathbf{q}_1, \mathbf{q}_2)$ of the sampled image $S(\mathbf{q})$ is equal to the covariance of the random process $e(\mathbf{x})$, $R_e(\mathbf{q}_1, \mathbf{q}_2)$.

2.2. B-spline image modeling

We look at the B-spline family of basis functions, where $\beta^0(\mathbf{x})$ is the centered, normalized, rectangular pulse and $\beta^n(\mathbf{x}) = \beta^{n-1} * \beta^0(\mathbf{x})$, while n refers to the degree of the basis function. Note that when $d > 1$, $\beta^n(\mathbf{x}) = \prod_{i=1}^d \beta(x_i)$. A continuous model for the sampled image may be obtained through

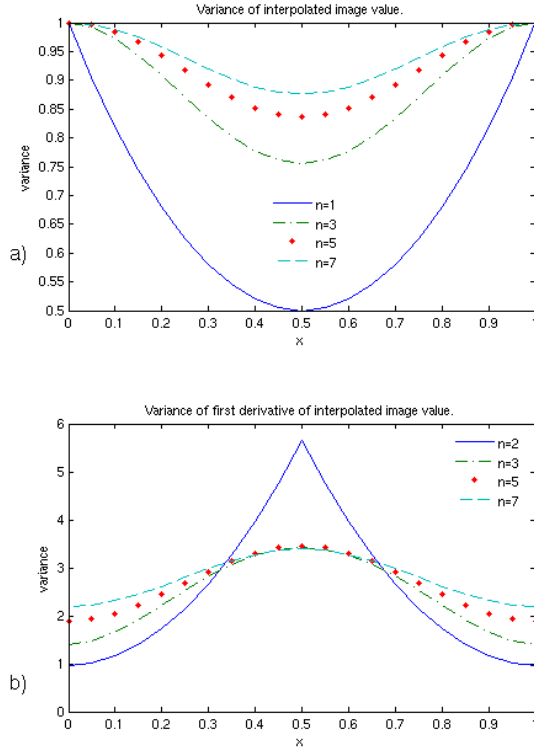


Fig. 1. Variance of a white noise discrete random process interpolated using B-splines of different degrees. Part (a): variance of random process itself as a function of spatial coordinate x . Part (b): variance of first derivative of random process made continuous with B-splines of different degrees.

a linear combination of basis functions $\beta^n(\mathbf{x})$:

$$\hat{S}(\mathbf{x}) = \sum_{\mathbf{i} \in \mathbb{Z}^d} c(\mathbf{i}) \beta^n(\mathbf{x} - \mathbf{i}), \quad (3)$$

where the coefficients $c(\mathbf{i})$ are obtained by solving a linear system. Alternatively, the continuous model can also be obtained through inverse filtering [1, 2] by:

$$\hat{S}(\mathbf{x}) = \sum_{\mathbf{i} \in \mathbb{Z}^d} S(\mathbf{i}) \eta^n(\mathbf{x} - \mathbf{i}) \quad (4)$$

where $\eta^n(\mathbf{x})$ is known as the cardinal B-spline interpolator and is given by:

$$\eta^n(\mathbf{x}) = \sum_{\mathbf{k} \in \mathbb{Z}^d} (\beta^n)^{-1}(\mathbf{k}) \beta^n(\mathbf{x} - \mathbf{k}), \quad (5)$$

where $(\beta^n)^{-1}(\mathbf{k})$ is the uniquely defined convolution inverse [1, 2].

2.3. Covariance properties of interpolated signals

The covariance function of the interpolated image $\hat{S}(\mathbf{x})$ is given by:

$$R_{\hat{S}}(\mathbf{x}_1, \mathbf{x}_2) = \sum_{\mathbf{q}_1, \mathbf{q}_2 \in \mathbb{Z}^d} \eta^n(\mathbf{x}_1 - \mathbf{q}_1) R_S(\mathbf{q}_1, \mathbf{q}_2) \eta^n(\mathbf{x}_2 - \mathbf{q}_2). \quad (6)$$

If we are dealing with band-limited white noise, for example, the variance of an interpolated value $\hat{S}(\mathbf{x})$ is given by:

$$R_{\hat{S}}(\mathbf{x}, \mathbf{x}) = \sigma^2 \sum_{\mathbf{q} \in \mathbb{Z}^d} [\eta^n(\mathbf{x} - \mathbf{q})]^2, \quad (7)$$

where $\sigma^2 = R_e(\mathbf{x}, \mathbf{x})$. Similarly, the variance of a derivative of $\hat{S}'(\mathbf{x})$ is:

$$R_{\hat{S}'}(\mathbf{x}, \mathbf{x}) = \sigma^2 \sum_{\mathbf{q} \in \mathbb{Z}^d} [(\eta^n)'(\mathbf{x} - \mathbf{q})]^2. \quad (8)$$

In Figure 1 we plot equations (7) and (8), with $\sigma^2 = 1$, for cardinal B-spline interpolators of several degrees for $x \in [0, 1]$. Note that as the degree of the interpolator increases, $R_{\hat{S}}$ tends to σ^2 . This is to be expected since, as shown by Aldroubi *et al.* [3] $\eta^n(\mathbf{x}) \rightarrow \text{sinc}(\mathbf{x})$ as $n \rightarrow \infty$, and it is easy to show that $\sum_{\mathbf{q}=-\infty}^{\infty} [\text{sinc}(\mathbf{x} - \mathbf{q})]^2 = 1, \forall \mathbf{x}$.

3. APPLICATIONS

3.1. Sub-pixel image registration

Sub-pixel accuracy in image registration (alignment) is desirable, since many biological structures of interest, for example, are of the size of a pixel or so. Moreover, in applications where it is necessary to estimate rotations, and general elastic transformations, one has no choice but to use a strategy that estimates the values of the images in locations which were not originally sampled.

To demonstrate the effects of low degree interpolation on image registration methods, we look at the following example. A source image $S(\mathbf{q})$, with $\mathbf{q} \in \mathbb{Z}^2$ organized in an $M \times M$ grid, is translated with respect to a target image $T(\mathbf{q})$ by

$$\hat{S}(\mathbf{q} - \mathbf{t}) = \sum_{\mathbf{i} \in \mathbb{Z}^d} S(\mathbf{i}) \eta^n(\mathbf{q} - \mathbf{t} - \mathbf{i}), \quad (9)$$

where $\mathbf{t} = \{t, 0\}$ is a simple translation vector in one dimension of the image. Note that this is a simple linear operation on the intensity values of the images. Thus, if we write \mathbf{S} to represent the digital image $S(\mathbf{q})$ in vector notation, a translated version of the same image can be computed with a linear operation $\mathbf{F}_t \mathbf{S}$, with the values of \mathbf{F}_t determined by the equation above. At each translation value, the discrete 2-norm of the difference between the target and translated source images is used to measure the alignment between the images. The value t for which the discrete 2-norm is minimized is the

optimal translation value. In the context of the energy minimization framework described earlier, this translates to:

$$\Psi(S(f(\mathbf{q})), T(\mathbf{q}), f) = \|\mathbf{F}_t \mathbf{S} - \mathbf{T}\|^2 \quad (10)$$

where \mathbf{T} is the target image in vector notation, and $\|\mathbf{S}\|^2 = \frac{1}{M^2} \sum_{i=1}^{M^2} (S(\mathbf{q}_i))^2$.

Let $\mathbf{S} = \tilde{\mathbf{W}}_S + \mathbf{e}_S$ represent the vector of sampled image values (the vector notation for equation (2)). Similarly, let the target image in vector notation be $\mathbf{T} = \tilde{\mathbf{W}}_T + \mathbf{e}_T$. Inserting these into (10), the objective function being minimized becomes:

$$\|\mathbf{F}_t \mathbf{S} - \mathbf{T}\|^2 = \|\mathbf{F}_t \tilde{\mathbf{W}}_S - \tilde{\mathbf{W}}_T\|^2 + \|\mathbf{e}_T\|^2 + \|\mathbf{F}_t \mathbf{e}_S\|^2. \quad (11)$$

If the noise process is weakly stationary $\|\mathbf{F}_t \mathbf{e}_S\|^2$ is equivalent to a sample variance estimate, which, as shown in part a of Figure 1, oscillates according to equation (6) (equation (7) in the case of white noise):

$$\|\mathbf{F}_t \mathbf{e}_S\|^2 \approx R_{\hat{S}}(\mathbf{t}, \mathbf{t}). \quad (12)$$

Thus, computational algorithms that seek to optimize 10 are likely to converge to one of the many artificial local optima, instead of a 'true' solution.

The artifactual oscillations in the objective function can be reduced using zero degree B-spline interpolation (nearest neighbor). However, this is not advisable since sub-pixel measurements would not be possible. Oscillations can also be avoided by using a continuous 2-norm instead of the discrete one in (10). This, however, could be computationally impractical for all but the most trivial applications. Another alternative is to 'smooth' the image prior to computation of the cost function so as to minimize the oscillations in $\|\mathbf{F}_t \mathbf{e}_S\|^2$. This, however, is also not optimal since blurring can reduce edge information that can be critical for obtaining a good match. Finally, as shown in the results section, the magnitude of the oscillations can be decreased by increasing the degree of the B-spline interpolant.

3.2. Sub-pixel edge detection

Very similar arguments can be used to describe artificial oscillatory behavior in cost functions used to detect edges in noisy images. Let $f(s) = (f_x(s), f_y(s))$, $s \in [0, 1]$, be a curve in two dimensional space. Image edges can be detected by finding $f(s)$ such that a line integral following the path of $f(s)$ over a potential energy field derived based on image values is minimized. The potential energy is usually computed as the magnitude squared of the gradient estimated based on the image data. Mathematically,

$$\begin{aligned} \Psi(S(\mathbf{q}), \mathbf{f}) &= \int_0^1 \|\nabla \hat{S}(f(s))\|^2 ds \\ &\approx \sum_{i=1}^T \|\nabla \hat{S}(f(i\tau))\|^2, \end{aligned} \quad (13)$$



Fig. 2. Magnetic resonance image used for experimental results. For the results relating to sub-pixel edge detection, the white line shown towards the left of the figure was translated from left to right.

where τ is the distance between values s in the curve $f(s)$ and T is the total number of points being summed. As opposed to the registration example given above, equation (13) is maximized instead of minimized. Again using the image model (2), and assuming that the noise component is independent from the signal, the equation above can be simplified:

$$\Psi(S(\mathbf{q}), f) = \sum_{i=1}^T \|\nabla \tilde{W}(f(i\tau))\|^2 + \|\nabla e(f(i\tau))\|^2. \quad (14)$$

The term $\sum_{i=1}^T \|\nabla e(f(i\tau))\|^2$ again can be interpreted as a sample variance computation and depending on curve f and choice of τ can contain artificial oscillatory behavior. Again, a common choice is to 'blurr' the intensity value of the images prior to computations. By definition, however, this operation will reduce edge information. This is especially counterproductive since image edges are being sought. As shown in Figure 1, part b, another option to reduce the artificial oscillatory behavior is to increase the degree of the B-spline interpolant being used.

4. RESULTS

The results in this section were computed based on the MRI image of the human brain shown in Figure 2. This two dimensional image was taken from a realistic MRI simulator [4]. In the first example, the image was translated with respect to itself, at sub-pixel values, and the value of the discrete 2 norm between the original image and the translated image was measured for each translated value. The experiment was repeated using several of the B-spline interpolators aforementioned. As evident from the results shown in Figure 3, part a, low degree interpolators tend to produce objective functions that contain local optima indentations caused by interpolation on noise. As the degree of the B-spline increases, however,

5. DISCUSSION AND CONCLUSION

We've shown that B-spline-based extraction of geometric functions to sub-pixel accuracy is not possible when using low degree basis functions. In image registration problems the solution will be biased towards the most 'blurred' image, while in edge detection problems, the solutions will be biased towards half-pixel coordinates. The arguments used here to explain the local optima artifacts in registration curves can be expanded to include other cost functions (or similarity measures as they are called in the image registration literature) such as correlation and mutual information [5, 6].

Several strategies can be used for reducing the bias in the solutions. The most commonly used one is to reduce the influence of noise by low-pass filtering the input images prior to the computations. Increasing the degree of B-spline interpolators, as we have shown, can also help reduce the bias in the solutions obtained. Finally, ideal sinc interpolation can also be used to remove artifactual oscillations in the cost functions [5, 6]. In many useful circumstances sinc-type interpolation can be implemented efficiently using the fast Fourier Transform algorithm [6] for improved optimization.

6. REFERENCES

- [1] M. Unser *et al.*, "B-Spline Signal Processing: Part I-Theory," *IEEE Transactions on Signal Processing*, vol. 41, pp. 821-833, 1993.
- [2] M. Unser *et al.*, "B-Spline Signal Processing: Part II-Efficient Design and Applications," *IEEE Transactions on Signal Processing*, vol. 41, pp. 834-848, 1993.
- [3] A. Aldroubi *et al.*, "Cardinal spline filters: Stability and convergence to the ideal sinc interpolator," *Signal Processing*, vol. 28, pp. 127-138, 1992.
- [4] <http://www.bic.mni.mcgill.ca/brainweb/>
- [5] G.K. Rohde *et al.*, "Measuring image similarity in the presence of noise," In *Proceedings of the SPIE Medical Imaging: Image Processing*, San Diego, February 2005. pp 132-143.
- [6] G.K. Rohde, "Registration Methods for Quantitative Imaging," University of Maryland, College Park, Maryland, USA, 2005.

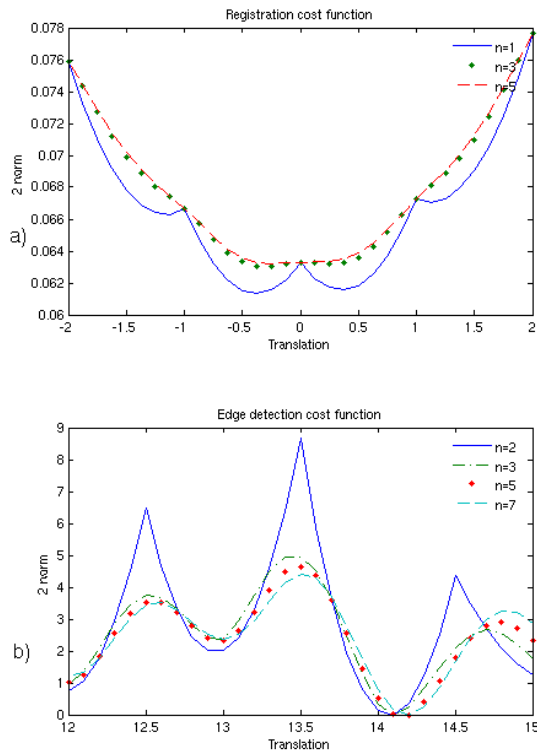


Fig. 3. Image registration (part a) and edge detection (part b) cost functions computed using the image shown in Figure 2 as the line was translated from left to right.

these artifacts are diminished and almost not noticeable when using B-splines of degree 5 or greater.

In a second experiment, the energy of the first derivative of the image was computed over a short straight line (white line shown in Figure 2) as the line was translated continuously from left to right. As can be seen from this figure, the line is placed on a background region whose intensity values are governed by system noise. Thus, ideally, the integral of image derivatives over the line should remain flat as the line is translated over background regions. Fluctuations resulting from noise should be random, and, ideally, no systematic local optima should occur. To remove random fluctuations in the value of the integral as the line is translated the image was smoothed with a 3x3 box filter prior to the computations. The experiment was repeated using the several B-spline interpolators described earlier. Results are shown in Figure 3, part b. As seen from these results, cost functions computed using low degree interpolators contain systematic local optima artifacts. As the degree of the B-spline increases, the magnitude (height of the bumps) of such artifacts decreases.